

²⁶C. J. N. van den Meijdenberg, K. W. Taconis, and R. de Bruyn Ouboter, *Physica* **27**, 197 (1961).

²⁷J. R. Clow and J. D. Reppy, *Phys. Rev. Letters* **16**, 887 (1966).

²⁸R. F. Harris-Lowe and K. A. Smee, *Phys. Rev. A* **2**, 158 (1970).

²⁹M. F. Collins, V. J. Minkiewicz, R. Nathans, L.

Passell, and G. Shirane, *Phys. Rev.* **179**, 417 (1969).

³⁰A. Tucciarone, L. M. Corliss, and J. M. Hastings, *J. Appl. Phys.* **42**, 1378 (1971).

³¹In the two-fluid model of superfluid helium the superfluid density is identified with the square of the order parameter (see for example, Ref. 21).

Induced Compton Scattering and Nonlinear Propagation in Laser-Created Plasmas

M. Decroisette, J. Peyraud, and G. Piar

*Commissariat à l'Energie Atomique, Centre d'Etudes de Limeil,
94-Villeneuve-Saint-George, France*

(Received 2 April 1971)

We have obtained some evidence of the induced scattering of an electromagnetic wave by Compton collisions, and of its nonlinear propagation in a plasma. The interpretation of the modified spectral profile of the interacting radiation is compatible with plasma parameters.

I. INTRODUCTION

In 1933, Kapitza and Dirac suggested that electrons might be scattered by stationary light waves such as by using a diffraction grating.¹ We present this experiment in another form, without standing waves and where energy exchanges are possible. Let us focus a laser beam, i. e., a high radiative-energy flux, on a plasma by means of a lens. Besides ordinary Compton collisions, in which a photon is absorbed and reemitted spontaneously with a frequency shift in some given direction, the stimulated Compton effect must be taken into account. In fact, some scattered photons may belong to the incoming light in direction and in energy, because of the solid angle Ω and the spectral linewidth $\Delta\nu$ of the incident beam (Fig. 1). According to the quantum theory of radiation, they will be stimulated by the incoming photons and thus the scattering observed in the direction of the laser beam will be enhanced.

In our experiment, where the plasma is highly inhomogeneous and reflecting, for the incoming

laser light, the photon distribution can be considered nearly isotropic. Then it is possible to calculate the transfer of energy from photons to electrons, and the mean shift of the spectral profile towards the lower frequencies.

In the present paper, Sec. II is devoted to a theoretical investigation of stimulated Compton scattering effects in a plasma, Sec. III to the experimental setup, and Sec. IV to the interpretation of the experimental results.

II. THEORETICAL CONSIDERATIONS

It has been shown that the Compton electron-photon interaction can be described in a kinetic theory by a Boltzman-like interaction operator (Refs. 2 and 3). The only difference from the classical Boltzmann operator is due to the boson nature of photons which introduces induced terms.

Let us note $\vec{\nu} = \Omega\vec{\nu}$, the vector frequency of a photon and $N(\vec{\nu})$, the photon distribution in frequency space. [If we deal with polarized photons we have to introduce the two functions $N^i(\vec{\nu})$, $i=1, 2$ according to the polarization.] The propagation equation, taking into account Compton effects, is

$$\left(\frac{\partial}{\partial t} + c\vec{\Omega} \frac{\partial}{\partial \vec{x}}\right) N^i(\nu) = c \int \sigma \{ [N^i(\nu') + c^3 N^i(\nu) N^i(\nu')] f(p') - [N^i(\nu) + c^3 N^i(\nu') N^i(\nu)] f(p') \} d\Omega' d\vec{p}, \quad (1)$$

where $f(\vec{p})$ is the electron distribution function.

For unpolarized photons $N^1(\vec{\nu}) = N^2(\vec{\nu}) = \frac{1}{2}N(\vec{\nu})$. The equation for the total density $N(\vec{\nu})$ is the same as Eq. (1) except for the replacement of c^3 by $\frac{1}{2}c^3$ in front of $N(\vec{\nu})N(\vec{\nu}')$.

It can be shown² that $\sigma d\Omega'$ takes the value

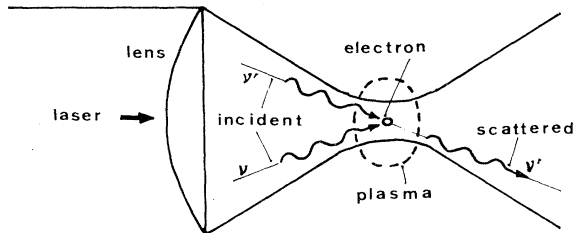


FIG. 1. Schematic diagram of stimulated Compton scattering.

$$\sigma d\Omega' = \frac{\epsilon_0}{\epsilon} \frac{\nu_0}{\nu} \sigma(\nu_0, x_0) d\Omega_0$$

$[\sigma(x)$ is the classical Compton cross section for the x deflection $\sigma = \frac{1}{2}(r_0^2)(1 + \cos^2 x)$ (r_0 is the classical electron radius)], where the 0 subscript pertains to quantities measured in the Gallilean system in which the total momentum is zero. ϵ_0 , ν_0 , x_0 are, respectively, the total energy, the frequency of the photon, and the deflection angle.

The operator on the right-hand side of Eq. (1) can be expanded in term of the small parameter p/mc , where p is the electron momentum and m the rest mass of the electron. Let us summarize some typical results of Ref. 4.

In zeroth order, only the photon angular deflection is described, the electrons staying at rest. In this order the photon gas obeys the simple Lorentz equation

$$\frac{d^{(0)}}{dt} N(\vec{\nu}) = n_e c \int \sigma(x) [N(\nu\vec{\Omega}) - N(\nu\vec{\Omega}')] d\Omega',$$

while the electron distribution remains unchanged $[(d^{(0)}/dt)f(\vec{p}) = 0]$.

In the first order it is the radiation-pressure effect on the electrons which is described through the relation

$$\frac{d^{(1)}}{dt} f(\vec{p}) = -\sigma_e n_e \int h\nu\vec{\Omega} N(\nu\vec{\Omega}) d\nu \frac{\partial f(\vec{p})}{\partial \vec{p}} dp$$

($\sigma_e = \frac{8}{3}\pi r_0^2$, total Compton cross section).

In second order the interaction between distribution functions is described. A kinetic temperature for the photon gas is introduced. Provided the photons are isotropic, the kinetic temperature is given by

$$kT_\phi = \frac{1}{4} \frac{\int (h\nu)^2 [N(\nu) + \frac{1}{2}c^3 N^2(\nu)] d\nu}{\int h\nu N(\nu) d\nu}$$

for unpolarized photons.

The electron and photon distribution functions obey, respectively, the relations

$$\begin{aligned} \frac{d^{(2)}}{dt} f(\vec{p}) &= \frac{4}{3} c\sigma_0 \frac{u}{mc^2} \\ &\times \left(3f(\vec{p}) + \vec{p} \frac{\partial f(\vec{p})}{\partial \vec{p}} + mkT_\phi \Delta_{\vec{p}} f(\vec{p}) \right) \end{aligned}$$

(u is the radiative energy density and $\Delta_{\vec{p}}$ is the Laplace operator in \vec{p} space) and

$$\begin{aligned} \frac{d^{(2)}}{dt^2} N(\nu) &= n_e c\sigma_0 \frac{h\nu}{mc^2} \frac{1}{\nu^3} \frac{d}{d\nu} \\ &\times \left[\nu^4 \left(N(\nu) + \frac{1}{2}c^3 N(\nu) + \frac{k\bar{T}_e}{h} \frac{d}{d\nu} N(\nu) \right) \right] \end{aligned}$$

($\frac{3}{2}k\bar{T}_e$ is the average energy of an electron).

The energy transfer between electrons and photons is given by the very simple relation

$$\left(\frac{dw}{dt} \right)_{e \rightarrow \phi} = - \left(\frac{dw}{dt} \right)_{\phi \rightarrow e} = 4n_e \sigma_0 c \frac{u}{mc^2} (k\bar{T}_e - kT_\phi).$$

Obviously, for blackbody radiation $T_\phi = T \approx h\bar{\omega}$, but for nonequilibrium radiation such as laser radiation, the values of T_ϕ are such that $T_\phi \gg h\bar{\nu}$, and the energy transfer is greatly enhanced. In that case only the induced terms are important. For a stationary interaction roughly depending only on the x variable, it is convenient to consider the spatial distribution of the light intensity

$$I(\nu, x) = c\Omega_0 \nu^2 N(\nu) h\nu,$$

Ω_0 being the solid extension of the radiation.

Noting that $d/dt = c\Omega(\partial/\partial \vec{x})$ for a stationary interaction, the light intensity $I(\nu, x)$ obeys the relation

$$\frac{\partial}{\partial x} \frac{I(\nu, x)}{\nu} = \frac{\mu}{4\pi} \Omega_0 n_e \frac{r_0^2}{m} \frac{\partial}{\partial \nu} \left(\frac{I(\nu, x)}{\nu} \right)^2 \quad (2)$$

in which Ω_0 is the solid angle of the laser beam, $I(\nu, x)$ is the spectral distribution of the light intensity $[I(\nu, x) = c\Omega_0 \nu^2 N(\nu) h\nu]$, and r_0 the classical radius of the electron. μ is a screening factor introduced in the same expansion as the one used for the kinetic equation; provided, it is not too small, it is given by

$$\mu = \text{Inf} \left\{ 2 \frac{mc^2}{kT_e} \left(\frac{\Delta\nu}{\nu} \right) \left(\frac{1}{\Omega_0} \right)^{1/2}, 1 \right\}. \quad (3)$$

In this expression Inf stands for "the smaller of the two values in the bracket."

Equation (2) is of the Korteweg-deVries type and yields multivalued solutions. In order to prevent this, we used a classical trick (used in many problems of nonlinear propagation)—add to it a term of the form $\partial^3/\partial \nu^3 [I(\nu, x)/\nu]$. From the classical discussions of the Korteweg-deVries equations (e.g., see Ref. 5) we are thus led to predict (a) a mean shift of the frequency profile towards the lower frequencies:

$$\partial \nu = -L \frac{2\mu}{4\pi} \Omega_0 n_e \frac{r_0^2}{m} \frac{I_0}{\Delta\nu}, \quad (4)$$

where L is the interaction length, I_0 the total intensity of the light flux, and $\Delta\nu$ its spectral width; and (b) breaking of the profile into secondary ones; these profiles are named "solitons," following the Korteweg-deVries literature terminology.

III. EXPERIMENT

We have tried to show some evidence of induced Compton scattering in an interaction experiment between a laser and a solid target.⁶ The plasma is obtained by focusing a laser beam by means of a plane aspheric lens ($f = 50$ mm, aperture $f/1$) inside a solid deuterium target which has a 4-mm² square cross section. The laser is a conventional Nd³⁺ glass laser, with a master oscillator and 5-

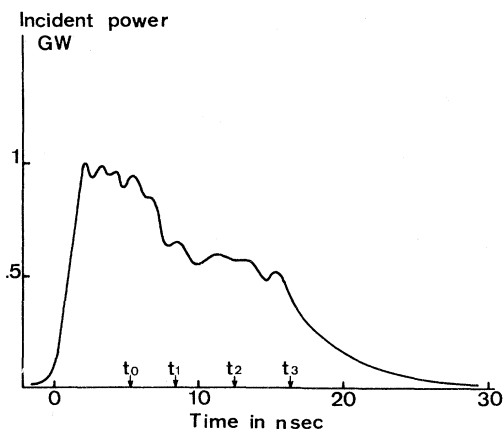


FIG. 2. Typical laser pulse.

rod cascade amplifier. The delivered pulse has a short rise time (≤ 5 nsec) and a half-width of 15-20 nsec. We worked with a peak power of 1 GW (Fig. 2) and a mean energy of 10 J (in the focal volume, the flux was $\approx 10^{12}$ W/cm²).

Under these conditions, the typical plasma parameters are: electron density of 10^{20} to 10^{21} cm⁻³ and electron temperature of a few hundred electron volts.⁷

A. Experimental Setup

1. Principle

The setup enabled us to observe the modification of the transmitted spectral profile, resolved in time as the spectrum was changing in the course of time with plasma evolution. Thus a photomultiplier attached to a monochromator was used rather than a photographic device. The spectral profiles were thus obtained point by point. Because of this shot-by-shot procedure, reproducibility of the experimental conditions had to be checked for each shot. In particular, the total energy and power in the laser radiation, its spectral position, and the plasma evolution were part of the routine measurements performed for each shot and these tests are described in detail in Sec. III A 3.

We had to ascertain that the observed phenomenon was not due to a change in the spectrum of the incident radiation—before its interaction with the plasma—and that any observed spectral change was present in the plasma scattered laser light only. In particular, the polarization of the plasma scattered laser light was to be that of the incident laser beam and was not of plasma emission origin, which, if any at the laser light wavelength (or near), should be largely unpolarized.

Therefore, the spectra of the incident and transmitted radiation had to be studied simultaneously with the spectrum of the plasma emitted light in a direction perpendicular to the laser beam, where

the induced effect is expected to be unobservable.

In order to avoid three identical instruments for this purpose, these spectra were separated by appropriate optical delays.

2. Description

The laser beam is focused by means of the lens O_1 (Fig. 3). The transmitted photons impinge then on the lens O_2 , which is set to make an afocal system with O_1 . The transmitted beam is reflected by the mirrors M_1 , M_3 , M_4 , and the semitransparent slab S ; it is then focused across a polarizer (glan prism) on the entrance aperture F of a grating Ebert-Fastie monochromator and detected using a photomultiplier. A small fraction of the incident energy is also sent onto the monochromator by reflections on slabs V_3 , V_4 on mirror M_2 , M_3 , M_4 and on slab S . The perpendicular emission of the plasma is focused across S on F by means of the lens L_1 . At the exit of the monochromator the spread is 15 \AA mm^{-1} . The entrance and exit slit widths are 0.5 mm. The average wavelength of the spectral region under study is determined within an accuracy of 0.1 \AA . Two cells observe the transmitted and incident pulses. A calibrated calorimeter—not shown in Fig. 3—exposed to a well-determined fraction of the laser beam, allows us to record the total incident energy. At last the creation and growth of the plasma is followed by a streak-camera recording.

The signals were recorded in the sequence illustrated by the insert in Fig. 3: a signal for incident pulse evolution control (PI); a signal for plasma emission given by the photomultiplier, resolved in time and in wavelength (EP), the shift of 40 nsec with respect to PI arises from the transit time of the photomultiplier; two signals also delivered by the photomultiplier, for the transmitted (RT) and incident (RI) laser lines, time and wavelength re-

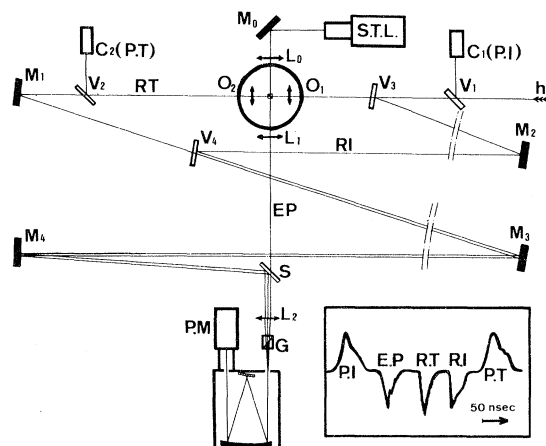


FIG. 3. Experimental setup.

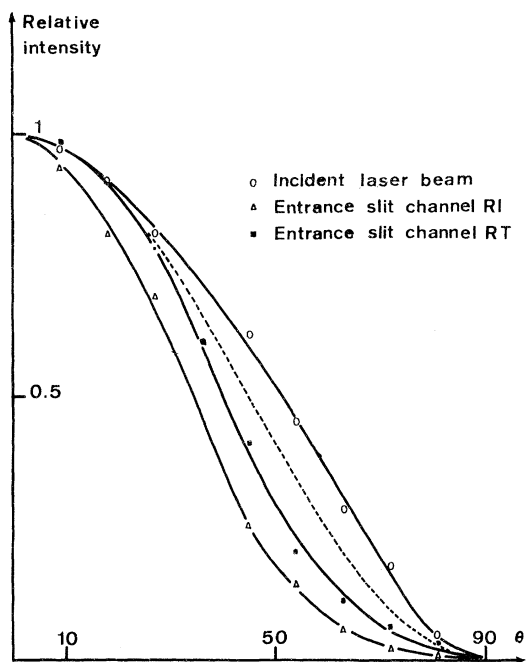


FIG. 4. Study of the polarization.

solved also, and for which the optical delay lines set respective shifts of 60 and 120 nsec with respect to EP; and a signal for transmitted pulse evolution control (PT) electrically 300 nsec shifted with respect to PI.

3. Tests

Shot-to-shot reproducibility of the plasma history and of the laser-beam focalization inside the target (at 1.6 mm behind the front face of the ice) were checked by means of streak photographs.⁷

Reproducibility of the laser shots was checked by three signals: (a) the signal CAL given by the calorimeter, due to the error on this measurement, the energy was kept at the same level ± 0.5 J from one shot to the other; (b) the signal PI indicating the laser power output, for the same reasons mentioned previously, the power was determined to ± 0.2 GW; and (c) the signal RI for which an experimental error of 10% led to an uncertainty of 3 Å on the wavelength measured in the line wing (the profile shape is preserved during an hypothetical wavelength shift which would be undetected by either PI or CAL).

The error on the power measurement of the transmitted ray was also 10%. Every experimental point making up the curves shown in Figs. 7 and 8 is in fact an average performed over several shots. Shots which did not meet the maximum error requirements were not taken into consideration. The dispersion in the results is much lower than the systematic error.

Since the polarization of the different radiations was fundamental to our experiment, we studied the polarization of the laser beam at the exit of the last rod, and the depolarization due to the different reflections of the whole setup. In Fig. 4, three graphs represent the normalized transmitted energy vs glan tilting angle θ : at the laser output, at the monochromator entrance, channel RT, and channel RI. By comparison with the theoretical curve $I = \cos^2\theta$ (dotted line) it can be seen that the laser radiation is almost entirely polarized, and that the depolarization due to the optical setup is slight (depolarization factor $< 2\%$).

The long optical delay lines needed frequent realignments which were done by means of a He-Ne gas laser, but had the advantage to select only the rays striking the plasma core without any diaphragm. The amount of plasma transmitted light, first estimated at 10^{-2} by means of cells C_1 and C_2 , was more precisely valued close to 10^{-3} with the monochromator-photomultiplier system, by comparison with a shot without target.

In Fig. 5 the time history of the transmitted and incident pulses, at a wavelength $\lambda_0 = 10575$ Å, is shown with the two signals being balanced by means of neutral filters, and the laser pulse starting at time zero. The first peak in the transmitted signal corresponds to the foot of the incident one when the breakdown threshold was just reached ($t = -10$ nsec). This peak is not visible on the other graph because of the scale.

In Fig. 6 the power level of these peaks are plotted, and the times t_0 , t_1 , t_2 , t_3 when the signals were analyzed are reported.

B. Experimental Results

The first experiment was done under the follow-

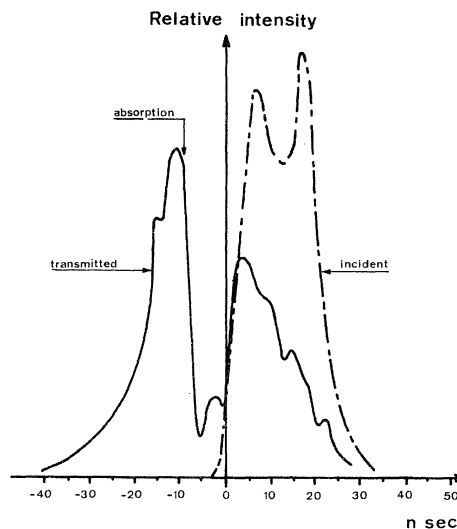


FIG. 5. Typical transmitted pulse.

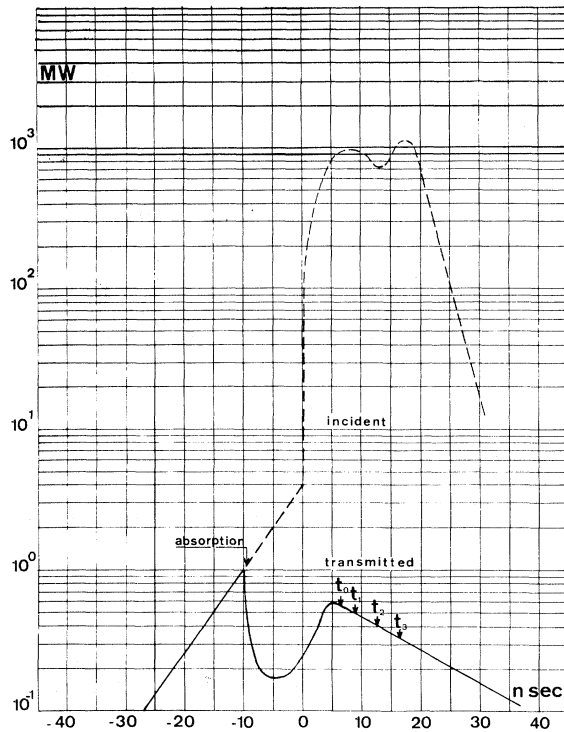


FIG. 6. Power of the incident and transmitted pulses.

ing conditions: $t = t_0 = 6 \pm 0.5$ nsec, energy = 14.5 ± 0.5 J, and peak power = 1.2 ± 0.2 GW.

In Fig. 7, the spectral profiles of transmitted and incident lines are plotted vs the wavelength shift $\Delta\lambda$ from λ_0 . The vertical scale is arbitrary. While the left-hand side of the transmitted profile remains unmodified, an important change has occurred on the right-hand side (the incident and transmitted relative intensities are matched at λ_0): The profile intensity decreases at $\lambda \approx 1.06 \mu$ and a second line appears shifted by nearly 45 \AA with respect to λ_0 . The preservation of the initial polarization was checked by means of a glan prism: Both lines are entirely polarized. The transmitted energy is 16 mJ, i. e., a power close to 1 MW for the main line and 0.2 MW for the second line.

In the same spectral region and at the same time ($t = 6$ nsec) the spectral profile observed in a direction perpendicular to the incident light is similar to the transmitted one and is also entirely polarized. However, it is much smaller in intensity by at least two orders of magnitude. In spite of their similarity, we shall see that these two spectra cannot be due to an emission-line process.

A more accurate chronology of the recorded signals was made afterwards with the following conditions: energy = 10 ± 0.5 J, peak power = 0.9 ± 0.2 GW, $t_1 = 8.5 \pm 0.5$ nsec, $t_2 = 12.5 \pm 0.5$ nsec, $t_3 = 16.5 \pm 0.5$ nsec. For these times the spectral

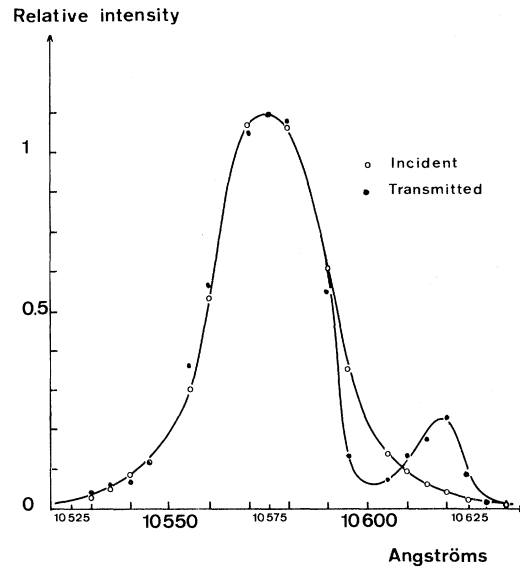


FIG. 7. Modification of the profile.

variations of the modified right-hand edge of the line have been plotted Fig. 8. As can be seen, rapid changes occur. Two secondary lines appear at first, shifted by 30 and 40 \AA respectively; then 4 nsec later, another one shows up. In the end, one peak only remains.

Moreover, as in the first study, the spectrum measured at 90° is similar to the transmitted one, except for the total power in the spectrum.

IV. INTERPRETATION

Three fundamental characteristics are observed: The phenomenon intensity is very large; the shift occurs towards longer wavelengths only; and the light polarization is preserved.

This effect cannot be due to any plasma line emis-

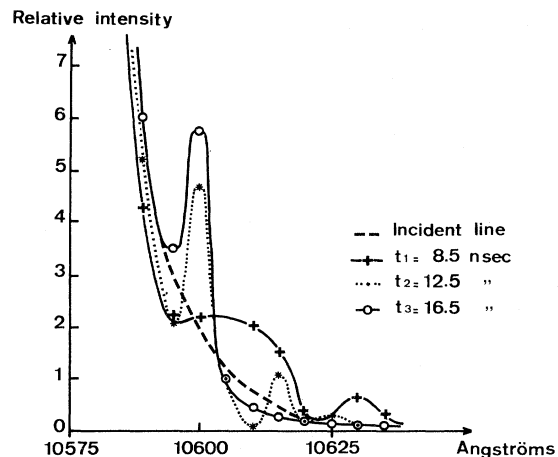


FIG. 8. Evolution of the transmitted line.

sion. Blackbody radiation at 1.06μ for $T_e = 100$ eV is equal to 0.3 W for an emitting surface of 10^{-3} cm^2 with a spectral width of 7 \AA . This figure is six orders of magnitude lower than the transmitted recorded intensity. Since no spontaneous emission can be more intense than blackbody radiation, it follows that the transmitted line is due to a stimulated effect; as for the spectrum observed at 90° , it may simply come from Fresnel reflection of the incident radiation profile—once modified by Compton effect (see further)—as it propagates through a variable refractive-index medium⁸. Neither can this effect be due to Thomson scattering, taking into account the small differential cross sections $\sigma_{\text{th}} = 8 \cdot 10^{-26}$ cm^2 and the following parameters:

$$n_e \approx 2 \cdot 10^{20} \text{ cm}^{-3}, \quad T_e \approx 100 \text{ eV}, \\ V = 10^{-5} \text{ cm}^3, \quad \Omega = 0.6 \text{ sr}.$$

The forward scattered power for this process is found to be $P_{\text{th}} \approx 0.5$ W. Nor can this effect be due to wave coupling of the incident wave to plasma longitudinal waves. For instance, by interaction with the incident wave, ion-acoustic waves are slow enough to give rise to a secondary transverse wave located in the observed spectral region. However, polarization would not be preserved and symmetric shifts should appear at wavelengths $\lambda_0 \pm \Delta\lambda$. This effect cannot be due to plasma motion, Doppler effect being invisible along the beam propagation direction.

On the contrary, induced Compton scattering explains satisfactorily the observed phenomenon. It gives a correct account of: (a) the polarization, well defined as in any scattering process; (b) the intensity, as already mentioned. Moreover, the preferential direction in which the phenomenon is

observed agrees with the hypothesis of an induced effect; and (c) the wavelength shift, in accordance with the measured plasma parameters [see Eq. (4) in which we have substituted $T_e = 100$ eV, $N_e = 2 \cdot 10^{20}$ cm^{-3} , $L = 200 \mu$].

It gives also a correct account of (a) the modified line's shape; the intensity decrease at $\lambda = 1.06 \mu$ is consistent with a number of photon conservation; and (b) the nonlinear aspect of its propagation, theoretically described by the Korteweg-deVries equation (3) and clearly shown in Fig. 8.

So, induced Compton scattering seems a valid interpretation.

V. SUMMARY AND CONCLUSION

In a laser-produced plasma, we have observed an induced phenomenon which preserves polarization, which shows a shift toward longer wavelengths and which propagates in a nonlinear fashion.

These characteristics are fully compatible with the induced Compton scattering theory. However, more experiments are necessary in order to conclude definitively on the origin of this phenomenon, and in particular to check the linear variation of the wavelength shift with I_0 , which is characteristic of any energy exchange between photons and electrons varying on I_0^2 .

Note added in manuscript. The first part of our experiment⁹ (Fig. 7) was also performed recently by I. K. Krasnyuk, P. P. Pashinin, and A. M. Prokhorov,¹⁰ but without any study of polarization.

ACKNOWLEDGMENTS

The authors wish to acknowledge the theoretical assistance of J. L. Bobin, P. Guillaneux, and D. Colombant.

¹P. L. Kapitza, P. A. M. Dirac, Proc. Cambridge, Phil. Soc. **29**, 297 (1933).

²H. Dreicer, Phys. Fluids **7**, 735 (1964).

³D. H. Sampson, *Radiative Contribution to Energy and Momentum Transport in Gas* (Interscience, New York, 1965).

⁴J. Peyraud, J. Phys. (Paris) **29**, 306 (1968); **29**, 872 (1968).

⁵J. J. Zabuský and M. D. Kruska, Phys. Letters **15**, 240 (1961).

⁶J. L. Bobin, F. Delobea, G. de Giovanni, C. Fauquig-

non, and F. Floux, Nucl. Fusion **9**, 115 (1969).

⁷C. Colin, Y. Durand, F. Floux, D. Guyot, and P. Langer, J. Phys. (Paris) Suppl. **29**, C3 (1968).

⁸R. G. Tomlinson, IEEE J. Quantum Electron. **5**, 591 (1969).

⁹M. Decroisette, G. Piar, and F. Floux, Phys. Letters **32A**, 249 (1970).

¹⁰J. K. Krasnyuk, P. P. Pashinin, and A. M. Prokhorov, Zh. Eksperim. i Theor. Fis. Pis'ma v Redaktsiyu **12**, 439 (1970) [Sov. Phys. JETP Letters **12**, 305 (1971)].